ANALYSIS AND DESIGN OF THIN PLANAR ABSORB-ING STRUCTURE USING JERUSALEM CROSS SLOT

H. X. Liu[*], B. F. Yao, L. Li, and X. W. Shi

School of Electronic Engineering, Xidian University, Xi'an 710071, China

Abstract—A detailed analysis and design of thin planar absorbing structure using Jerusalem cross slot (JCS) is presented in this paper. Based on uniplanar compact high-impedance surface characteristics, the resistance loss material layer can be directly attached to the surface of JCS structure, thus absorbing electromagnetic waves effectively. The improved design is characterized by its wider bandwidth and adjustable range. The absorption frequency band can be flexibly adjusted by the slot parameters. The influences of various structure parameters of JCS, including incident wave polarization and variation of incident angles on the absorption properties, are analyzed to provide guidance on theoretical design for practical application. The loaded resistance can be adjusted to obtain the optimum absorbing performance. The validation and effectiveness of the proposed design are conducted by using X-band waveguide simulation and measurement.

1. INTRODUCTION

Radar absorbing material (RAM) is a kind of special material which can absorb the incident electromagnetic wave and greatly reduce radar cross section (RCS). Salisbury screen is one of the most popular classical electromagnetic absorber design techniques [1]. This structure is composed of a resistive metallic screen and a ground plane separated by a quarter wavelength distance, with a dielectric between them to form the simplest resonant absorbing sandwich structure. However, the disadvantages of the screen are its narrow band and large thickness of an isolation layer of $\lambda/4$. Therefore, it is most desirable to find alternative designs which can lead to much thinner absorbers with high performance.

Artificial electromagnetic materials, such as frequency selective surface (FSS) [2], photonic band gap (PBG) structures [3–5], and left-handed materials [6, 7] are broadly classified as metamaterials, which are typically created by using two- or three-dimensional periodic metallic and dielectric structures. They have attracted significant research interest in recent years due to their special electromagnetic properties [8–10], which are widely applicable to antennas and microwave devices [11, 12]. The absorbing frequency band is expanded by replacing the traditional Salisbury screen with FSS [2, 13, 14]. It has been shown by Engheta [15] that there is the possibility of existing thin absorbing screens using metamaterial surfaces. Kern and Werner [16] in 2003 designed a new ultra-thin absorber based on electromagnetic bandgap metamaterials by utilizing a genetic algorithm to optimize the pattern. Gao et al., proposed a novel ultra-thin RAM employing the mushroom-like EBG structure [17]. The absorption mechanism and polarization sensitivity of ultra thin absorbers were discussed and analysed in [18–24].

Based on a uniplanar compact high-impedance (UC-HIS) structure, this paper proposes an improved design of thin planar absorbing structure using Jerusalem cross slot (JCS). The in-phase reflection characteristics support that the resistance loss material layer can be directly attached to the surface of UC-HIS structure. By parameter analyses, the influences of the various structural parameters of JCS, the polarization and incident angles of the incident electromagnetic wave, and loaded resistors on the absorbing properties are studied in depth. The correctness of the design of novel absorbing material is effectively validated by X-band waveguide simulation and measurement.

2. THEORETICAL ANALYSIS AND DESIGN

The major work of designing the absorbing material is to deal with two problems: one is how to maximize the incident electromagnetic wave into the material instead of reflecting off, and the other is how to attenuate the electromagnetic waves which enter into the material effectively. The former is essentially the impedance matching problem of absorbing material, and the latter is the attenuation characteristic of the material. Generally speaking, the two aspects are correlative dependence and interaction. The field reflection coefficient of the Salisbury screen is given as follows [1]:

$$R = \frac{j(1-\beta_1)\sin k_1 d_1 - Y_1(1-\alpha_1)\cos k_1 d_1}{j(1+\beta_1)\sin k_1 d_1 + Y_1(1+\alpha_1)\cos k_1 d_1} e^{j2k_0 d_1}, \qquad (1)$$

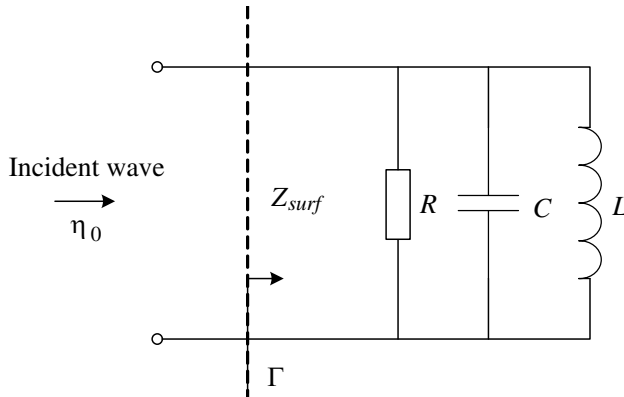**Figure 1.** The absorbing equivalent circuit of high impedance surface.

where α_1 and β_1 are the normalized complex magnetic surface impedance and electric surface admittance of the Salisbury screen. k_1, Y_1 and d_1 are the dielectric wave number, characteristic admittance and thickness of Salisbury screen, respectively.

It is known that 2D planar EBG structures have high impedance surface characteristics [8–10]. We use this kind of structures to construct in-phase reflection screen, on which electrical loss materials are loaded. By adjusting the resistance of electrical loss material, the equivalent surface impedance of the whole structure can approach to the wave impedance of free space, thus achieving the effectiveness of absorption. The absorbing equivalent circuit of the high impedance surface is shown in Fig. 1, in which equivalent inductance L and equivalent capacitance C deriving from the topology itself of HIS structures and form a parallel resonant circuit. The resistor R contains dielectric loss and loaded resistance loss. The calculation of reflection coefficient of the structure is shown in formula (2), in which Z_{surf} denotes the equivalent surface impedance of the absorbing structure and approximates a pure resistance at the resonant frequency, and η_0 is the wave impedance in free space.
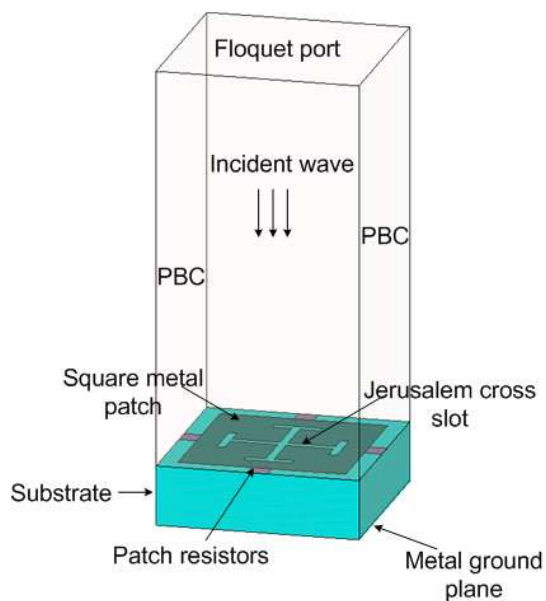
$$\Gamma = \frac{Z_{surf} - \eta_0}{Z_{surf} + \eta_0} \tag{2}$$

2.1. Design of Absorbing Structure with JCS

In this paper, we present a new thin planar absorbing structure with JCS, as shown in Fig. 2(a). The infinite periodic element of the absorbing structure with JCS is simulated by using the model shown
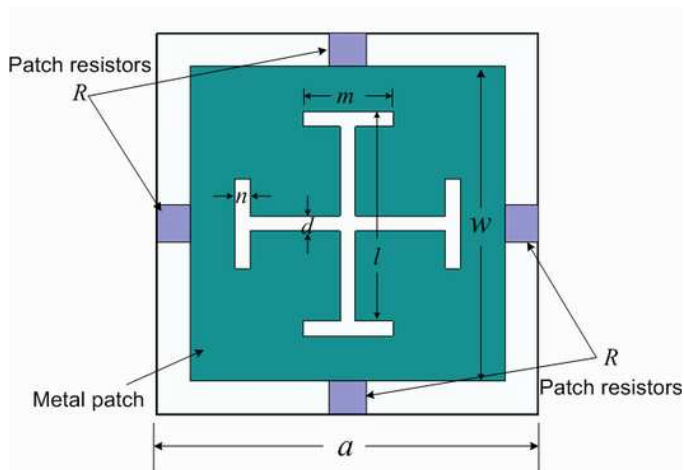
(a)

(b)

Figure 2. (a) Geometry of JCS. (b) Simulation model of infinite periodic element of absorbing structure using JCSin which the periodic boundary conditions (PBC) are put around the JCS cell.

in Fig. 2(b), around which periodic boundary conditions and Floquet port are set. The dielectric substrate is set as metal ground plane. a is the unit period and w is the width of square metal cell. The JCS has the slot width of d and n, and the slot length l and m. The loaded resistances R are set at four sides symmetrically. The relative permittivity and thickness are $\varepsilon_r = 4.4$ and $h = 1.5$ mm, respectively.

The initial parameter values are

$$a = 5.08 \, \text{mm}, \quad w = 4.2 \, \text{mm}, \quad d = 0.2 \, \text{mm},$$
$$n = 0.2 \, \text{mm}, \quad l = 3.0 \, \text{mm}, \quad m = 1.2 \, \text{mm}, \quad R = 266 \, \text{Ohm}, \quad (3)$$

which are used as a reference length to define the physical dimensions of the various JCS absorbing structures studied in this paper. HFSS full-wave simulation [25] is used to obtain amplitude and phase characteristics of reflection coefficient of a plane wave with normal incidence, as shown in Fig. 3.
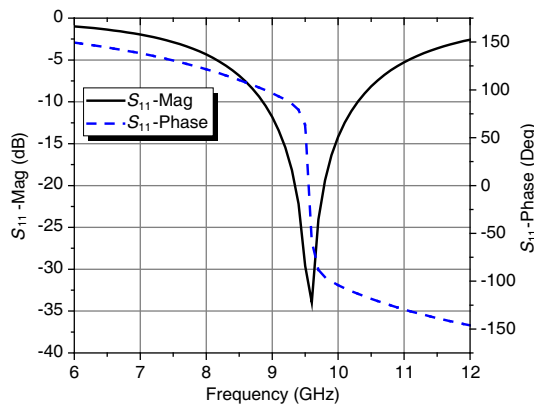
Figure 3. Reflection coefficient characteristics of Jerusalem cross slot absorbing structure versus frequency.

It can be seen that the absorbing peak of the structure is in accordance with the reflection phase zero-point, which takes on the characteristic of a magnetic wall. After adding appropriate lumped loss resistors, the reflection coefficient reduces to -30 dB below at the central frequency, which shows that the better absorbing effect can be achieved and the absorption bandwidth depends on band gap of JCS structure. Zero-point of reflection phase is approximately 9.6 GHz, and the relative bandwidth is about 15.1%. Compared with the structure using mushroom-like screen proposed by [16], the absorbing frequency band is wider and the unit size is smaller.

2.2. Parameters Analysis

In this section, we will discuss the effect of different values of JCS structure parameters on the absorbing performance, such as width of slot (d and n), length of slot (l and m), width of square metal patch (w), substrate thickness (h) and permittivity (ε_r), and loaded resistance (R).

2.2.1. Slot Length Effect

Slot length plays an important role in determining the absorbing frequency band. To study the effect of the JCS length, other parameters are kept the same as in (3). First, the slot length l is changed from 2.7 mm to 3.6 mm. Fig. 4 shows that the characteristics of reflection coefficient and equivalent surface impedance of absorbing structures with different slot length l.

The results show that zero-point of reflection phase which is the same as absorbing peak, shifts to lower frequency with the increase of JCS length l, i.e., from 9.7 GHz to 9.0 GHz. When l is changed as 2.7, 3.0, 3.3, and 3.6 mm, the corresponding values of magnitude of S_{11} are $-26, -34, -31$, and -23.5 dB, respectively. It is shown in Fig. 4(c) that the equivalent surface impedance Z_{surf} of JCS reduces as increasing JCS length l from 418 to 332 Ohm. When $l = 3.0$ mm, Z_{surf} is so closed to η_0 that absorption effect is the best. It is worthwhile to point out that a sudden change of the phase of S_{11} occurs when $l = 3.3$ mm
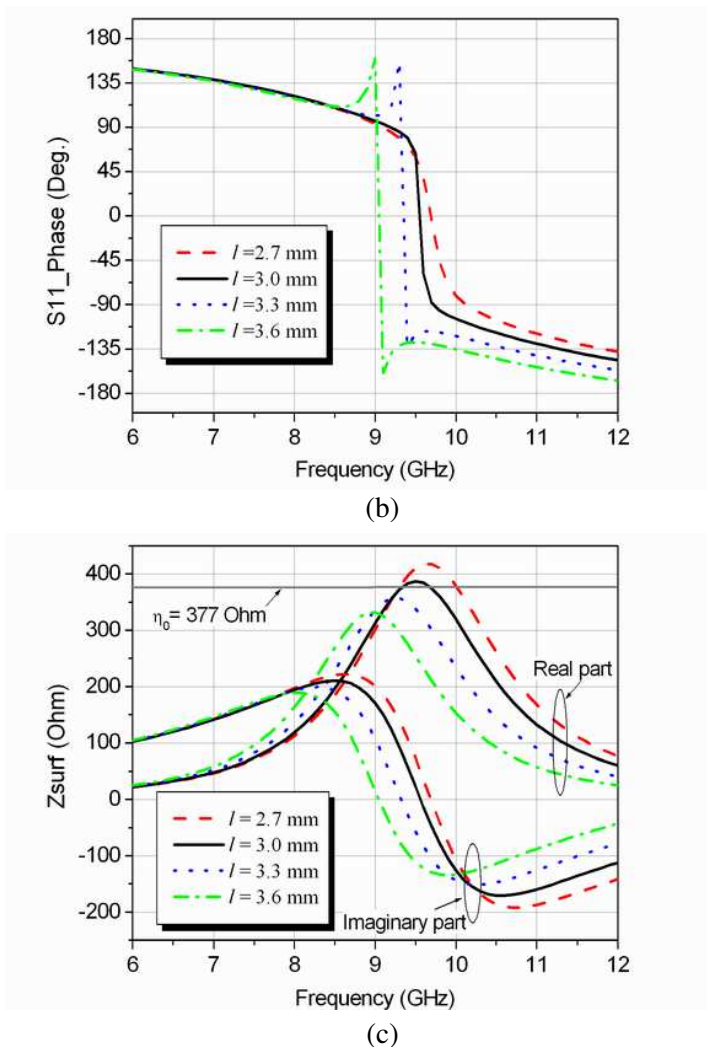

(a)

(b)

(c)
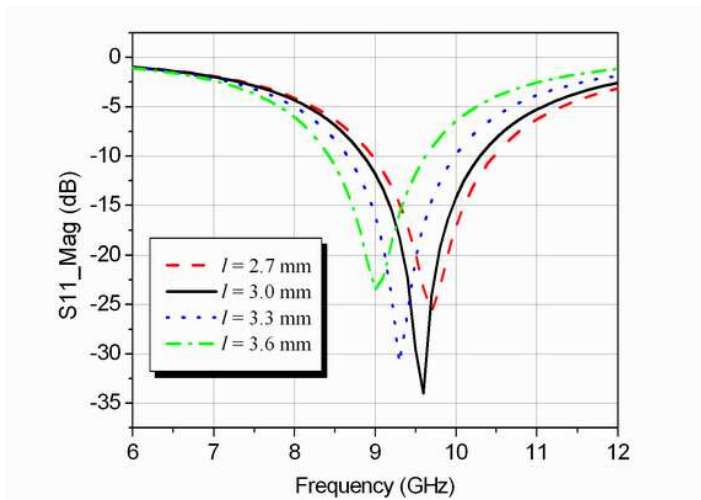
Figure 4. (a) Amplitude of Reflection coefficient. (b) Phase of reflection coefficient, and (c) equivalent surface impedance versus JCS length l.

and 3.6 mm. The reason is that the surface equivalent impedance Z_{surf} of the absorbing structure is less than wave impedance η_0 in those cases. Therefore, a smooth phase curve of reflection coefficient can be obtained as long as the value of surface equivalent impedance Z_{surf} is under control. Similar phenomena can be found in other parameters

analyses.

Second, the length m of JCS is changed as 1.2, 1.4, 1.6, and 1.8 mm, respectively. The reflection coefficient and effective surface impedance of absorbing structures varies with m, as shown in Fig. 5. It can be seen that the effect of m is the same as l, the resonant frequency will decrease from 9.6 to 9.0 GHz with m increasing from 1.2 to 1.8 mm. When $m = 1.4$ mm, Z_{surf} is best match with η_0 so that the maximum absorption can be obtained.

2.2.2. Slot Width Effect

When the width d of Jerusalem cross slot is set as 0.2, 0.4, 0.6, and 0.8 mm, respectively, the magnitudes of S_{11} of the absorbing structures are shown in Fig. 6(a). It can be seen that there is only a slight fluctuation, which means that the d of JCS has a little influence on the absorbing properties.

While the width n of Jerusalem cross slot is set as 0.2, 0.4, 0.6, and 0.8 mm, respectively, the resonant frequency shifts to lower frequency from 9.6 GHz to 9.4 GHz, as shown in Fig. 6(b).

2.2.3. Square Metal Cell Effect

The width of square metal patch w is an important parameter to determine the absorbing frequency range. When other parameters are kept the same as (3), and the cell size is changed from 3.8 to 4.4 mm, which is restricted by the period of JCS, the reflection coefficients of JCS absorbing structures with different w are shown in Fig. 7. The results show that the zero-point of reflection phase corresponding to absorbing peak will shift to lower frequency with the increase of square metal cell size w, i.e., from 10.8 to 8.9 GHz. The relative bandwidth has a little decrease from 15.7% to 14.3%.

2.2.4. Loaded Resistance Effect

The loaded resistance R should be adjusted to get the optimum absorbing property. The reflection coefficient of absorbing structure will vary when load resistance R is set as 226, 246, 266 and 286 Ohm, respectively, as shown in Fig. 8(a). It can be seen that the loaded resistor used to adjust the impedance match and dissipate power does not affect the resonant frequency of the absorbing structure that is only determined by JCS geometry parameters. Fig. 8(b) shows that surface equivalent impedance Z_{surf} increases from 334 to 420 Ohm as the increase of load resistor R, When $R = 266$ Ohm, Z_{surf} is so

matched with the wave impedance of free space that a minimum value of amplitude of reflection coefficient can be gained.

When $R = 0\,\mathrm{Ohm}$ which is a short circuit and equivalent to a small metal film connected adjacent cells, the structure would take on a total reflection, as shown in Fig. 9(a). In terms of the equivalent surface
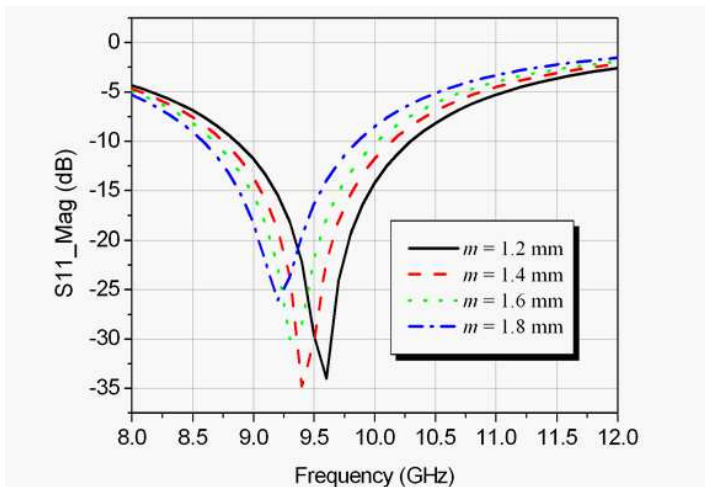
(a)
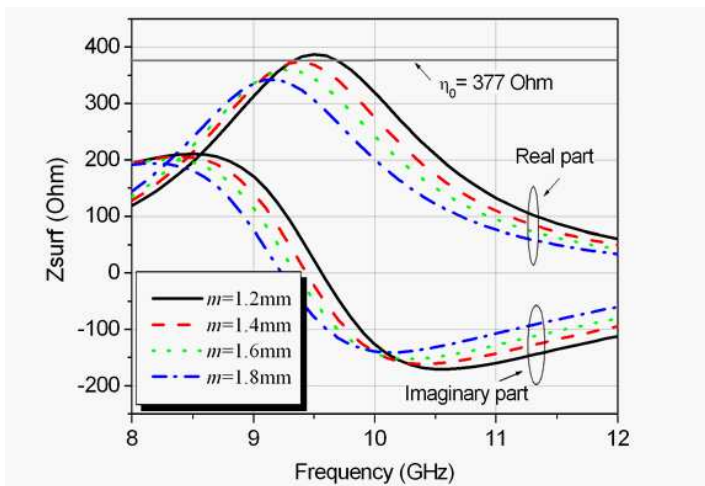
(b)

Figure 5. (a) Reflection coefficient curve. (b) Effective surface impedance of variation with JCS length m.

impedance in this case, the real part approaches zero and the imaginary part takes on a high admittance near resonant frequency, as shown in Fig. 9(c). If $R = 5000$ Ohm, the structure would be an open circuit and equivalent to coupling capacitive connection between adjacent cells. When the structure is resonant, it appears almost total reflection, and the surface impedance is a large real resistance. Therefore, even if
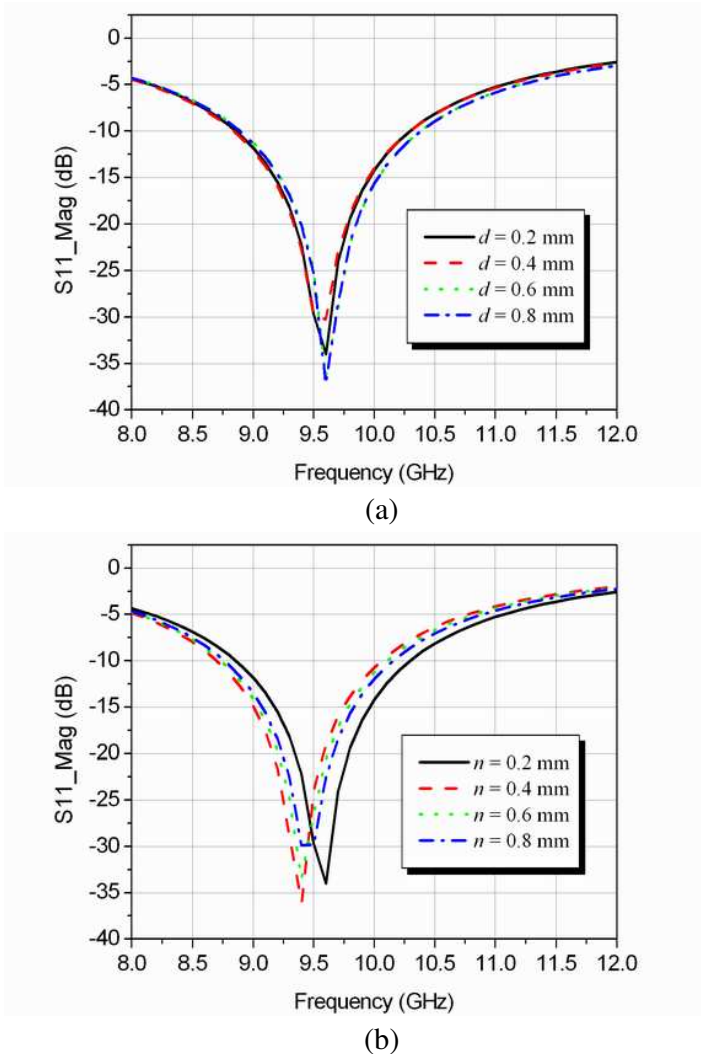

(a)

(b)

Figure 6. Reflection coefficient variation with JCS width d and n.

the large loss resistor is loaded, the effective absorption performance would not be achieved, due to mismatching. But the reflection phase characteristics also appear in-phase reflection property in the two situations, which are the equivalent magnetic conductor characteristics of UC-HIS structure, as shown in Fig. 9(b).
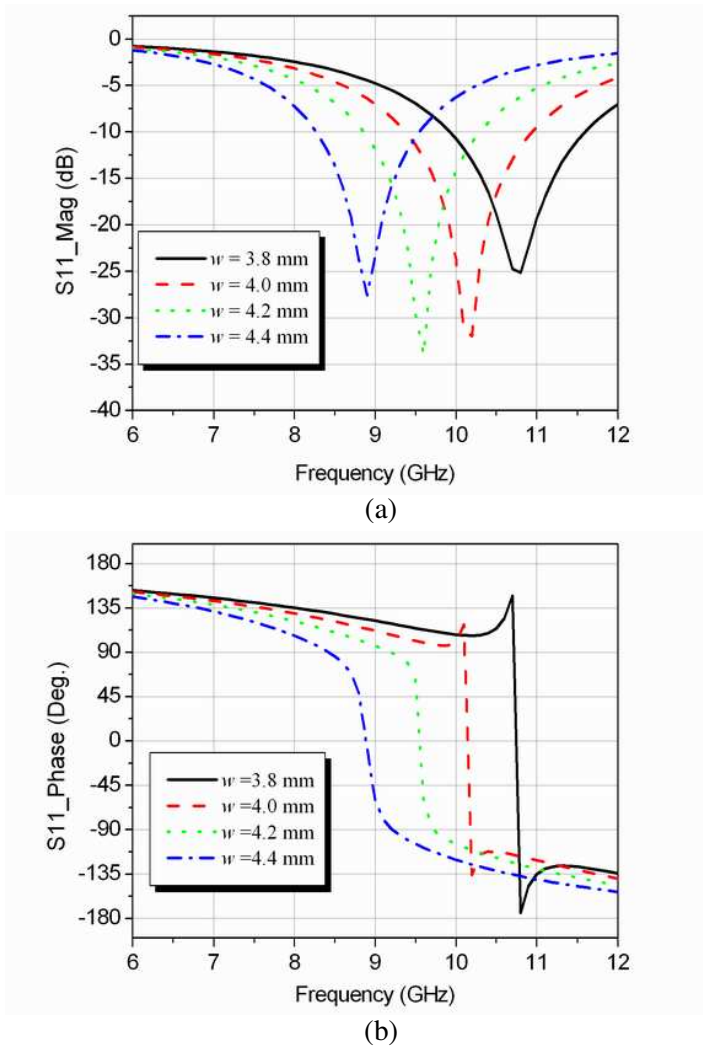

(a)

(b)

Figure 7. Reflection coefficient variation with the width of square metal patch w.
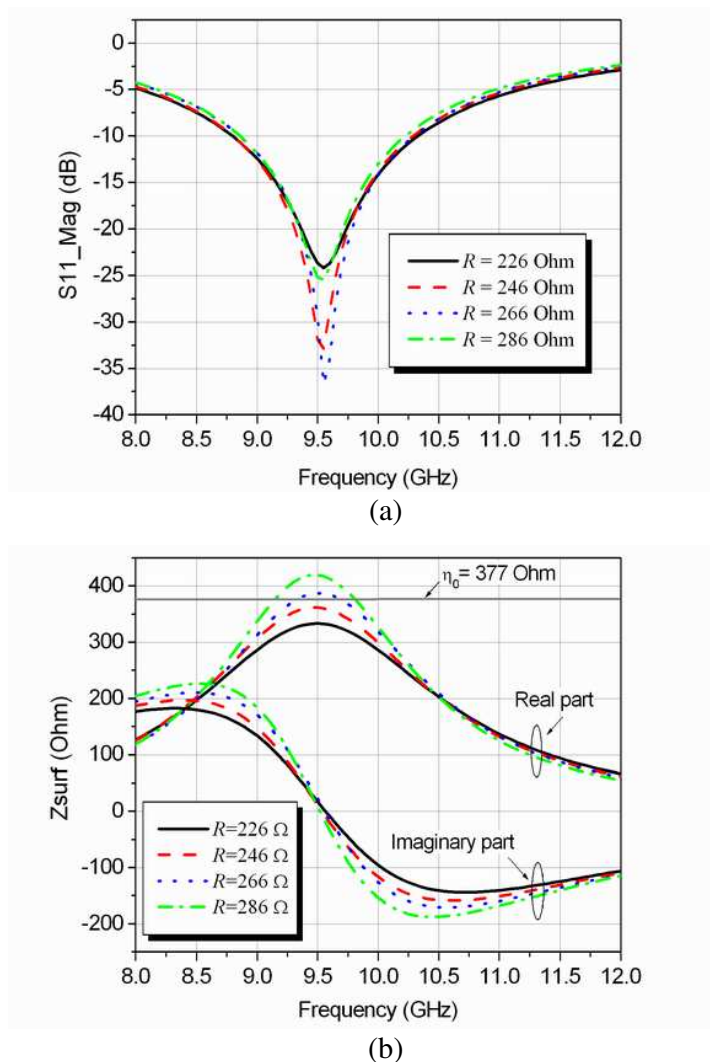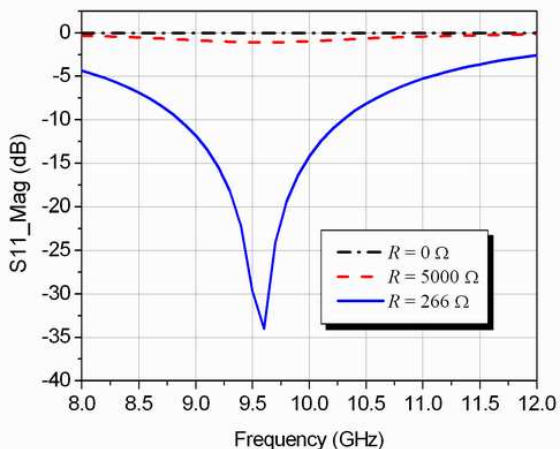
(a)

(b)

Figure 8. (a) Reflection coefficient curve of variation with load resistance R. (b) Effective surface impedance characteristics of variation with load resistance R.

## 2.2.5. Substrate Thickness and Permittivity Effect

It is significant to design a thin absorbing material. We analyse the effect of substrate thickness which is changed from 0.5 mm to 3.0 mm, when other parameters are kept the same as (3). It can be seen

from Fig. 10(a) that with the increase of thickness from 0.5 mm to 3.0 mm, the resonant frequency decreases from 11.7 GHz to 6.6 GHz remarkably, and the absorbing relative bandwidth increases from 3.2% to 21%. The results also show that the reflected magnitudes of all cases are below -10 dB. It is worthwhile to point out that the absorbing performance can be improved by adjusting the geometry parameters of JCS or loaded resistor R. For example, when the substrate thickness is very thin ($h = 0.5$ mm, $0.02\lambda_0$), we can adjust the loaded resistor $R = 500$ Ohm to further reduce S_{11}.

In addition, the absorbing frequency band can be effectively adjusted by changing substrate permittivity. As shown in Fig. 10(b),
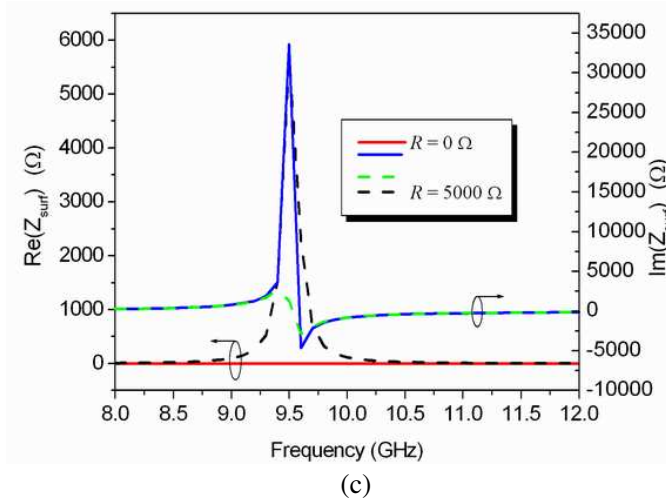

(a)

(b)

(c)
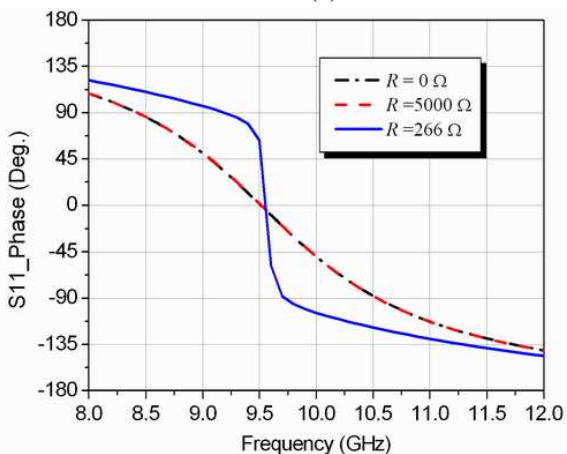
Figure 9. (a) Reflection coefficient amplitude of variation with load resistance R. (b) Reflection phase characteristics. (c) Surface equivalent impedance of variation with R.

the resonant band decreases with the increase of permittivity, as well as the bandwidth decreases.

3. ANALYSIS OF OBLIQUE INCIDENT PLANE WAVE

This paper takes into account the influence of various plane wave polarization and angles of incidence on absorbing characteristics of JCS. The structure parameters are selected as (3). First, TE polarized plane wave is oblique incident on the JCS structure. The incidence angles are set as $30°$, $45°$, and $60°$, respectively. The reflection coefficients of the JCS absorbing structure are shown in Fig. 11. Similarly, the results corresponding to TM polarized plane wave incidence are shown in Fig. 11 for comparison. Compared with normal incidence ($\theta = 0°$) in Fig. 11, the absorbing peak shifts to high frequency in the case of both TE and TM polarization with the increase of incidence angles θ. The resonant frequency of TE polarized incidence increases from 9.6 to 9.9 GHz, but it increases from 9.6 to 10.2 GHz for TM polarized incidence. The absorbing property of TE polarization is in accordance with that of TM polarization, which shows that the JCS has good polarization stability. However, when the incident angle is larger than 60 deg, the JCS absorbing structure does not work well.
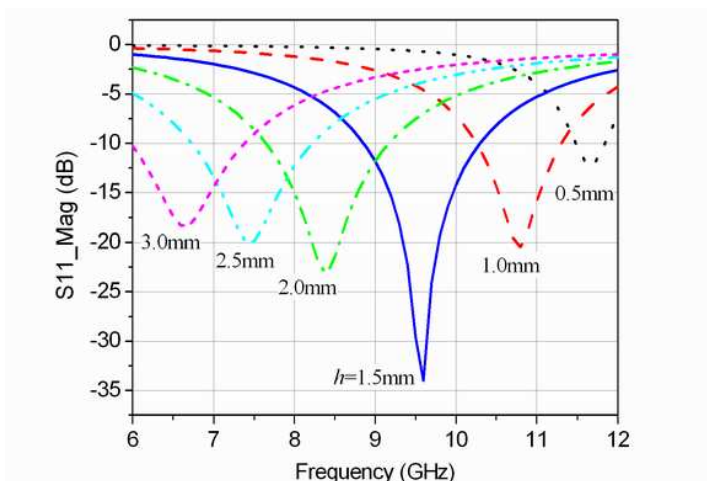
(a)
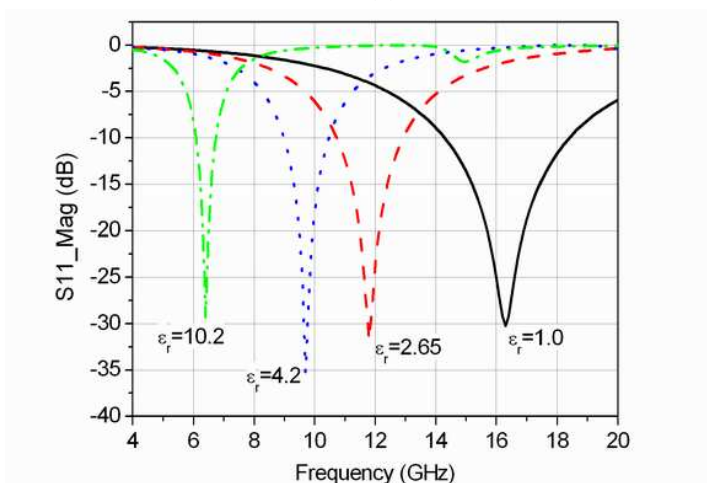
(b)

Figure 10. Reflection coefficient variation with (a) substrate thickness effect, (b) substrate permittivity effect.

4. WAVEGUIDE SIMULATION AND EXPERIMENTAL VERIFICATION

In order to validate the design of the absorbing material using JCS, the simple and effective waveguide simulation and measurement are performed in this paper. X-band standard rectangular waveguide
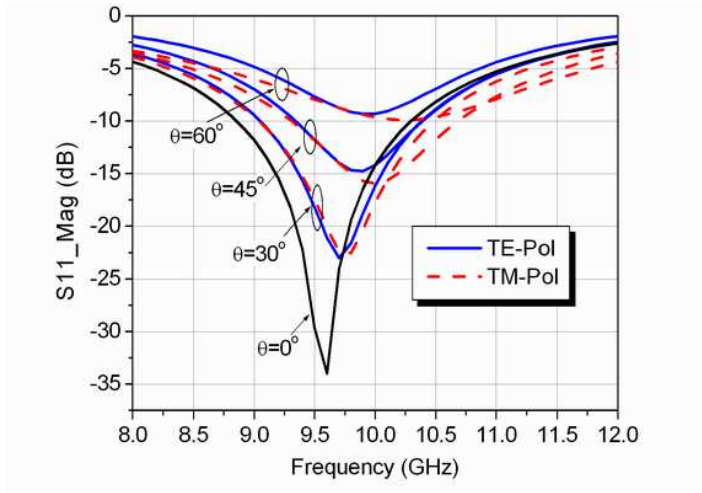
Figure 11. Reflection coefficients characteristics when TE and TM polarized plane wave oblique incidence on JCS absorbing structure.

(WR90) is used, and the dimensions of WR90 waveguide are $W_a = 22.86$ mm and $W_b = 10.16$ mm. According to the size of waveguide structure, we conducted an optimization design for the absorbing structure consisting of 2×4 Jerusalem cross slot cells. The unit period $a = 5.0$ mm, square metal cell $w = 4.16$ mm, JCS width $d = n = 0.22$ mm, JCS length $l = 2.98$ mm and $m = 1.18$ mm, loaded resistance $R = 280$ Ohm. The relative permittivity $\varepsilon_r = 4.6$ and thickness $h = 1.5$ mm. The waveguide simulation model is shown in Fig. 12(a), and the simulation result of S_{11} of the JCS absorbing structure is shown in Fig. 12(c). It can be seen that the designed JCS structure has a good absorbing characteristics.

To verify the absorbing phenomenon, a JCS plate with 4×2 cells was fabricated to perform a waveguide experiment. In order to match the inner aperture of WR90 exactly, a small dielectric fringe is added to the test sample. After calibration, we connected the waveguide to a port of Agilent vector network analyser Agilent 8719ES, and mount the absorber which with the same size exactly as the inner aperture of waveguide into the port of the waveguide, as shown in the Fig. 12(b). A waveguide-coaxial adaptor is used to measure S_{11} of the JCS absorber, and cover the port with a metal plate tightly to prevent any leaky waves. The measurement result is also shown in Fig. 12(c).

It can be seen that the zero-point of reflection phase of finite periodic unit structure shifts to higher frequency compared with that

of infinite periodic unit structure, which is caused by the finite periodic unit boundaries and TE-polarized oblique incidence in the waveguide measurement. The absorbing properties can be improved by increasing the number of periodic unit. The agreement of the simulation results with the experiment results verified the practicability and credibility of the model. The equivalent incident angle in the waveguide experiment is

$$\theta = 90^\circ - \cos^{-1}\left(\frac{\lambda}{2w_a}\right) \tag{4}$$

where λ is operating wavelength, w_a is broadside of the waveguide. When working frequency is 9.7 GHz, the equivalent angle of incidence in the waveguide in testing is $\theta = 42.6^\circ$. Setting the angle of incidence in the infinite periodic model as $\theta = 42.6^\circ$, we calculated the reflection coefficient and added in Fig. 12(c). The results show that zero-point of reflection phase of simulation model in the waveguide is agreement with that of infinite periodic model, except that the amplitude of reflection coefficient has an offset error that is caused by the finite periodic unit boundaries in waveguide experiment.
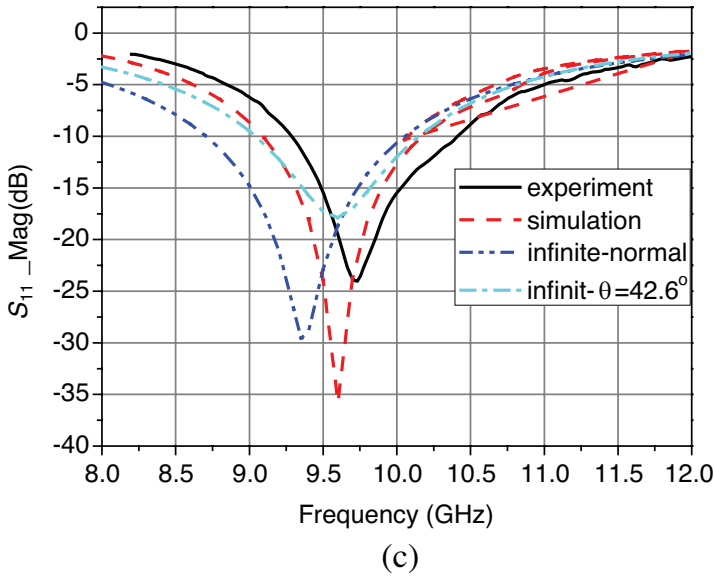

(a)

(b)

(c)
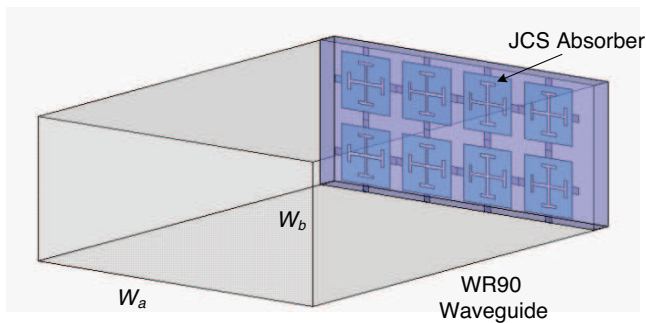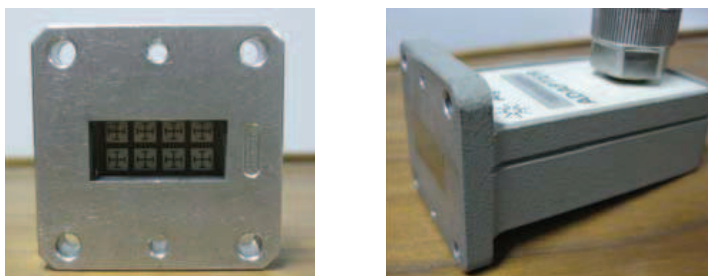
Figure 12. (a) Waveguide simulation model. (b) Test sample is mounted in the port of a waveguide, and a waveguide-coaxial adaptor for S_{11} measurement of the JCS absorber. (c) Comparison of measurement results with simulation results in waveguide model, in which the results calculated by using infinite periodic model for normal incidence and oblique incidence ($\theta = 42.6°$) are also given for comparison.

5. CONCLUSION

In this paper, a detailed analysis and design of thin planar absorbing structure with Jerusalem cross slot based on UC-HIS is proposed. The influence of structure parameters of JCS on absorbing characteristics is studied deeply. The absorbing frequency band is determined by the resonant frequency of JCS structure. The loaded resistor can be directly attached to the surface of JCS which is significantly used to adjust the matching and absorption ratio. The JCS absorbing structure has the advantages of wider bandwidth and adjustment parameters, which is helpful to practical applications. Finally, the accuracy and effectiveness of the proposed JCS structure design was validated by a simple and effective waveguide simulation and measurement.

ACKNOWLEDGMENT

REFERENCES

1. Fante, R. L. and M. T. McCormack, "Reflection properties of the salisbury screen," *IEEE Trans. Antennas and Propagat.*, Vol. 36, No. 10, 1443–1454, 1988.

2. Tennant, A. and B. Chamber, "A single-layer tuneable microwave absorber using an active FSS," *IEEE Microwave and Wireless Components Letters*, Vol. 14, No. 1, 46–47, 2004.

3. Yablonovitch, E., "Inhibited spontaneous emission in solid-state physics and electronics," *Phys. Rev. Lett.*, Vol. 58, 2059–2062, 1987.

4. John, S., "Strong localization of photons in certain disorded dielectric superlattices," *Phys. Rev. Lett.*, Vol. 58, 2486–2489, 1987.

5. Johnson, S. G. and J. D. Joannopuulos, *Photonic Crystals: The Road from Theory to Practice*, Kluwer Academic Publishers, Norwell, 2002.

6. Pendry, J. B., "Negative refraction makes a perfect lens," *Phys. Rev. Lett.*, Vol. 85, No. 18, 3966–3969, Oct. 2000.

7. Shelby, R. A., D. R. Smith, and S. Schultz, "Experimental verification of a negative refractive index of refraction," *Science*, Vol. 292, 77–79, Apr. 2002.

8. Yang, F. R., K. P. Ma, and T. Itoh, "A uniplanar compact photonic band-gap (UC-PBG) structrue and its applications for microwave circuits," *IEEE Trans. Microw. Theory Tech.*, Vol. 47, No. 8, 1509–1514, 1999.

9. Sieverpiper, D., L. Zhang, R. F. J. Broas, N. G. Alexopolus, and E. Yablonovitch, "High-impedance electromagnetic surfaces with a forbidden frequency band," *IEEE Trans. Microwave Theory Tech.*, Vol. 47, 2059–2074, Nov. 1999.

10. Li, L., Q. Chen, Q. W. Yuan, C. H. Liang, and K. Sawaya, "Surface-wave suppression band gap and plane-wave reflection

phase band of mushroomlike photonic band gap structures," *Journal of Applied Physics*, Vol. 103, 023513, Jan. 2008.

11. Yang, F. and Y. Rahmat-Samii, "Reflection phase characterizations of the EBG ground plane for low profile wire antenna applications," *IEEE Trans. Antennas Propagat.*, Vol. 51, 2691–2703, Oct. 2003.

12. Li, L., C. H. Liang, and C.-H. Chan, "Waveguide end-slot phased array antenna integrated with electromagnetic bandgap structure," *Journal of Electromagnetic Waves and Application*, Vol. 21, No. 2, 161–174, 2007.

13. Seman, F. C., R. Cahill, V. F. Fusco, and G. Goussetis, "Design of a Salisbury screen absorber using frequency selective surfaces to improve bandwidth and angular stability performance," *IET Microw. Antennas Propag.*, Vol. 5, No. 2, 149–156, 2011.

14. Yao, B., L. Li, and C. H. Liang, "An improved design of absorbing structure with Jerusalem cross slot," *The 9th International Symposium on Antennas, Propagation, and EM Theory*, Guangzhou, China, Nov. 29–Dec. 2, 2010.

15. Engheta, N., "Thin absorbing screens using metamaterial surfaces," *IEEE-APS International Symposium*, San Antonio, Texas, Jun. 16–21, 2002.

16. Kern, D. and D. Werner, "A genetic algorithm approach to the design of ultra-thin electromagnetic bandgap absorbers," *Microwave Opt. Tech. Lett.*, Vol. 38, No. 1, 61–64, Jul. 2003.

17. Gao, Q., Y. Yin, D. B. Yan, and N. C. Yuan, "Application of metamaterials to ultra-thin radar-absorbing material design," *Electronics Letters*, Vol. 41, No. 17, 1311–1313, 2005.

18. Kazemzadeh, A. and A. Karlsson, "On the absorption mechanism of ultra thin absorbers," *IEEE Trans. Antennas and Propagat.*, Vol. 58, No. 10, 3310–3315, 2010.

19. Costa, F., A. Monorchio, and G. Manara, "Analysis and design of ultra thin electromagnetic absorbers comprising resistively loaded high impedance surfaces," *IEEE Trans. Antennas and Propagat.*, Vol. 58, No. 5, 1551–1558, 2010.

20. Luukkonen, O., F. Costa, A. Monorchio, and S. A. Tretyakov, "A thin electromagnetic absorber for wide incidence angles and both polarizations," *IEEE Trans. Antennas and Propagat.*, Vol. 57, No. 10, 3119–3125, Oct. 2009.

21. Zhu, B., Z. Wang, C. Huang, Y. Feng, J. Zhao, and T. Jiang, "Polarization insensitive metamaterial absorber with wide incident angle," *Progress In Electromagnetics Research*,

Vol. 101, 231–239, 2010.

22. Li, M., H.-L. Yang, X.-W. Hou, Y. Tian, and D.-Y. Hou, "Perfect metamaterial absorber with dual bands," *Progress In Electromagnetics Research*, Vol. 108, 37–49, 2010.

23. Munir, A. and V. Fusco, "Effect of surface resistor loading on high-impedance surface radar absorber return loss and bandwidth," *Microwave and Optical Technology Letters*, Vol. 51, No. 7, 1773–1775, 2009.

24. Rozanov, K. N., "Ultimate thickness to bandwidth ratio of radar absorbers," *IEEE Trans. Antennas and Propagat.*, Vol. 48, No. 8, 1230–1234, 2000.

25. High Frequency Structure Simulator, Ansys Corporation.